Article

Magnetic and Optical Bistability Driven by Thermally and Photoinduced Intramolecular Electron Transfer in a Molecular Cobalt–Iron Prussian Blue Analogue

Dongfeng Li, Rodolphe Clrac, Olivier Roubeau, Etienne Hart, Corine Mathonire, Rmy Le Bris, and Stephen M. Holmes

J. Am. Chem. Soc., **2008**, 130 (1), 252-258 • DOI: 10.1021/ja0757632

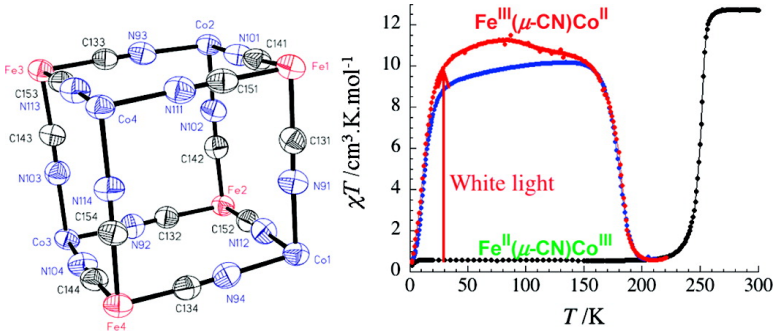

More About This Article

Additional resources and features associated with this article are available within the HTML version:

- Supporting Information
- Links to the 5 articles that cite this article, as of the time of this article download
- Access to high resolution figures
- Links to articles and content related to this article
- Copyright permission to reproduce figures and/or text from this article

View the Full Text HTML

J|A|C|S
ARTICLES
Published on Web 12/13/2007

Magnetic and Optical Bistability Driven by Thermally and Photoinduced Intramolecular Electron Transfer in a Molecular Cobalt−Iron Prussian Blue Analogue

Dongfeng Li,[†] Rodolphe Clérac,*[,‡] Olivier Roubeau,[‡] Etienne Harté,[‡] Corine Mathonière,*[,||] Rémy Le Bris,[||] and Stephen M. Holmes*[,†]

Contribution from the Department of Chemistry, University of Kentucky, Lexington, Kentucky 40506-0055, Université Bordeaux 1, CNRS, Centre de Recherche Paul Pascal, UPR 8641, 115 avenue du Dr. A. Schweitzer, 33600 Pessac, France, and Institut de Chimie de la Matière Condensée de Bordeaux, Université Bordeaux 1, CNRS, UPR9048, 87 avenue du Dr. A. Schweitzer, 33608 Pessac, France

Received August 1, 2007; E-mail: smholm2@uky.edu; clerac@crpp-bordeaux.cnrs.fr; mathon@icmcb-bordeaux.cnrs.fr

Abstract: A soluble molecular analogue of photoresponsive Co/Fe Prussian blues is described within this report. As judged via a variety of spectroscopic, magnetic, and crystallographic methods, electron transfer within the octanuclear complex (below 250 K) converts paramagnetic red crystals into green diamagnetic ones. The color and magnetic changes are associated with the transformation of Fe^{III}_{LS}-CN-Co^{II}_{HS} units into Fe^{II}_{LS}-CN-Co^{III}_{LS} fragments in manner that is identical to that found for the $A_n[Co(OH_2)_{(6-6m)}][Fe(CN)_6]_m \cdot xH_2O$ (A_n = alkali metal cation) family of three-dimensional Prussian blues. Moreover, this intramolecular electron transfer can be quantitatively circumvented via rapid thermal quenching and reversed via simple white light irradiation at low temperatures. Remarkably the data suggests that thermally or photoinduced paramagnetic metastable phases are identical and exhibit long relaxation times that approach 10 years at 120 K.

Introduction

Over the past decade there has been considerable interest in the development of tunable molecule-based materials that exhibit bistability in their physical properties as a function of external stimuli. Under ideal conditions such materials may allow for the construction of energy-efficient, switchable molecule-based information storage or electronic devices, assuming that the molecules can be properly addressed in electronic circuits.[1,2]

In 1996, Hashimoto and co-workers[3] first described that reversible magnetization changes could be photochemically induced in a magnetic molecule-based Prussian blue analogue of $K_{0.14}Co[Fe(CN)_6]_{0.71} \cdot 4.93H_2O$ stoichiometry. The compound adopts a face-centered cubic structure consisting of Fe−CN−Co linkages and exhibits an intense metal-to-metal charge transfer absorption in the visible region, ascribed to the conversion of Fe^{II}−CN−Co^{III} to Fe^{III}−CN−Co^{II} units via electron transfer.[3] The electron transfer can be either thermally or photochemically initiated affording dramatic changes in the magnetic and optical properties exhibited by the lattice. For example, red light irradiation (660 nm) increases the ferrimagnetic ordering temperature from 16 to 19 K and a concomitant increase of the magnetization is observed. This effect is ascribed to the phototransformation of diamagnetic Fe^{II}_{LS} (low-spin, t_{2g}^6)-CN−Co^{III}_{LS} (low-spin, t_{2g}^6) units into paramagnetic Fe^{III}_{LS} (low-spin, t_{2g}^5)-CN−Co^{II}_{HS} (high-spin, $t_{2g}^5e_g^2$) ones, and can be reversed via blue light irradiation (450 nm) or heating of the sample above 150 K, affording $Fe^{III}_{LS}(\mu\text{-CN})Co^{II}_{HS}$ (Scheme 1) linkages.[3] At temperatures below ca. 150 K, most of the material contains diamagnetic $Fe^{II}_{LS}(\mu\text{-CN})Co^{III}_{LS}$ units.

Subsequent reports by Verdaguer and Hashimoto described that the photomagnetic behavior of these Co/Fe Prussian blues can be systematically tuned via alteration of the Co/Fe ratio present in the nonstoichiometric $A_n[Co(OH_2)_{(6-6m)}][Fe(CN)_6]_m \cdot xH_2O$ (A_n = alkali metal cation) lattices.[4−14] When $m < 1$, the

[†] University of Kentucky.
[‡] Université Bordeaux 1, Centre de Recherche Paul Pascal.
[||] Institut de Chimie de la Matière Condensée de Bordeaux, Université Bordeaux 1.

(1) Sato, O.; Tao, J.; Zhang, Y.-Z. *Angew. Chem., Int. Ed.* **2007**, *46*, 2152−2187.
(2) Dei, A. *Angew. Chem., Int. Ed.* **2005**, *44*, 1160−1163.
(3) Sato, O.; Iyoda, T.; Fujishima, A.; Hashimoto, K. *Science* **1996**, *272*, 704−705.
(4) Sato, O.; Ohkoshi, S.-I.; Hashimoto, K. *J. Appl. Phys.* **2002**, *92*, 4834−4836.
(5) Shimamoto, N.; Ohkoshi, S.-I.; Sato, O.; Hashimoto, K. *Inorg. Chem.* **2002**, *41*, 678−684.
(6) Sato, O.; Einaga, Y.; Iyoda, T.; Fujishima, A.; Hashimoto, K. *Inorg. Chem.* **1999**, *38*, 4405−4412.
(7) Escax, V.; Bleuzen, A.; Cartier dit Moulin, C.; Villain, F.; Goujon, A.; Varret, F.; Verdaguer, M. *J. Am. Chem. Soc.* **2001**, *123*, 12536−12543.
(8) Champion, G.; Escax, C.; Cartier dit Moulin, C.; Bleuzen, A.; Villain, F.; Baudelet, F.; Dartyge, E.; Verdaguer, M. *J. Am. Chem. Soc.* **2001**, *123*, 12544−12546.
(9) Bleuzen, A.; Lomenech, C.; Escax, V.; Villain, F.; Varret, F.; Cartier dit Moulin, C.; Verdaguer, M. *J. Am. Chem. Soc.* **2000**, *122*, 6648−6652.
(10) Cartier dit Moulin, C.; Villain, F.; Bleuzen, A.; Arrio, M.; Sainctavit, P.; Lomenech, C.; Escax, V.; Baudelet, F.; Dartyge, E.; Verdaguer, M. *J. Am. Chem. Soc.* **2000**, *122*, 6653−6658.
(11) Gawali-Salunke, S.; Varret, F.; Maurin, I.; Enachescu, C.; Malarova, M.; Boukheddaden, K.; Codjovi, E.; Tokoro, H.; Ohkoshi, S.-I.; Hashimoto, K. *J. Phys. Chem. B* **2005**, *109*, 8251−8256.

10.1021/ja0757632 CCC: $40.75

Scheme 1. Thermally and Photoinduced Interconversion of $Fe^{II}(\mu\text{-CN})Co^{III}$ and $Fe^{III}(\mu\text{-CN})Co^{II}$ Units

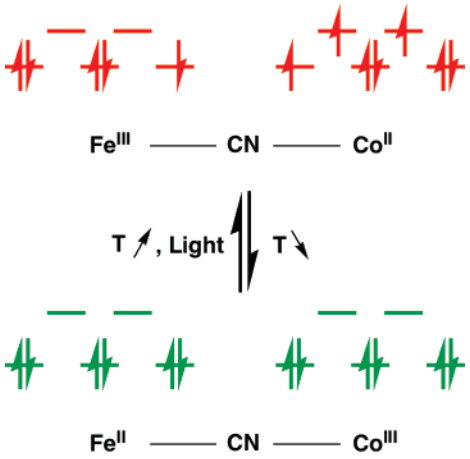

Fe sites are fractionally occupied and the Co centers concomitantly contain one or more water molecules to satisfy their coordination spheres. The number of coordinated water molecules, which is related to the number of low-spin $[Fe(CN)_6]^{3-}$ vacancies, act to tune the ligand field strengths and redox potentials of the Co centers; in these solids an average CoN_5O coordination environment and adjacent light-sensitive $[Fe(CN)_6]^{n-}$ sites are paramount for engineering lattices that exhibit reversible photoinduced magnetization changes.[1]

However while the optical and magnetic properties of Co/Fe Prussian blue analogues can be systematically tuned via stoichiometrically controlled alkali metal cation insertion, (resulting in defect lattices that are inherently nonstoichiometric), systematic structure−property studies become difficult at best. Therefore an active trend in cyanometalate research has been directed toward the synthesis of soluble and well-defined photoresponsive compounds via judicious choice of molecular building blocks. Using a building block synthetic strategy, self-assembly of cyanometalate anions and coordinatively unsaturated transition-metal cations can be utilized to generate discrete polynuclear products containing $Fe(\mu\text{-CN})Co$ linkages; examples include di-{FeCo},[15] tetra-$\{Fe_2Co_2\}$,[16] and penta-nuclear $\{Fe_2Co_3\}$[17−19] complexes, respectively. However, to the best of our knowledge, photomagnetic bistability has not been reported for these molecular complexes.

To this end, we have sought to prepare soluble molecular analogues of photoresponsive Prussian blues, using facially coordinate organic capping ligands to control the directionality and numbers of bridging cyanides and to mimic the cubic architecture of the lattice. In the present report we describe the structures, spectroscopic properties, and magnetic behavior of an octanuclear $\{Fe^{III}_4Co^{II}_4\}$ complex (**1**) that exhibits reversible intramolecular charge transfer as a function of temperature and light irradiation.

Experimental Section

Materials. All operations were conducted under an argon atmosphere by using standard Schlenk and drybox techniques. Transfers of solutions were carried out through stainless steel cannulas. Solvents were distilled under dinitrogen from CaH_2 (acetonitrile and dichloromethane), Mg turnings (methanol), or sodium-benzophenone (diethyl ether) and sparged with argon prior to use. Dimethylformamide (DMF) was dried using Linde 13X molecular sieves and sparged with argon before use. The preparation of K[pzTp],[20,21] $[(pzTp)_2Fe^{II}]$,[22] 2,2,2-tris(pyrazolyl)-ethanol,[23] $[NEt_4][(pzTp)Fe^{II}(CN)_3]$,[24] and $[NEt_4]CN$[25] are described elsewhere. $Co(ClO_4)_2\cdot 6H_2O$ (Baker) and aqueous 30% H_2O_2 (Aldrich) were used as received.

Physical Methods: IR and UV−Visible Spectroscopies. The IR spectra were recorded as Nujol mulls between KBr plates on a Mattson Galaxy 5200 FTIR instrument. UV−vis spectra were recorded under dinitrogen using a Shimadzu UV-2501 PC UV−vis recording spectrophotometer. Variable temperature IR and UV−vis data were collected using a liquid nitrogen cooled Graseby Specac Variable Temperature Cell (KBr windows) and controller operating between 77 and 300 K.

Physical Methods: Differential Scanning Calorimetry. Differential scanning calorimetry (DSC) measurements were conducted on a Perkin-Elmer Pyris apparatus using closed aluminum pans containing a polycrystalline sample of **1** (31.86 mg). Thermal equilibration was verified at the starting and final temperatures of each scan using 1 min isotherms with measurements repeated at various scan rates (10, 5, and 2 K min^{-1}). Temperature and enthalpy calibrations were performed using an indium reference sample. An average transition enthalpy of +56(4) kJ mol^{-1} was deduced via integration of the DSC peak after a polynomial baseline correction (Supporting Information, Figure S1, left, 2 K min^{-1}). Transition temperatures (254 K when cooling, 256 K when heating) were obtained by extrapolating the peak maxima temperatures to a zero scan rate (Supporting Information, Figure S1, right).

Physical Methods: Surface Reflectivity. The optical reflectivity properties of **1** under white-light irradiation (90(10) mW cm^{-2}) have been investigated using a home-built reflectivity system composed of a CVI spectrometer and three optical fibers: two for incident light (white light irradiation and analysis) and one for outgoing spectral analysis. The reflectivity signal was referenced to two standards: barium sulfate for the white color ($R = 1$, Abs. $= 0$) and activated charcoal for the black color ($R = 0$, Abs. $= 1$). This experimental setup allows for the collection of absorption spectra, between 500 and 900 nm in a temperature range of 10−290 K (3 K min^{-1}), while simultaneously observing the temperature dependence of the reflectivity signal at two different wavelengths (±2.5 nm). To avoid solvent loss, **1** was introduced into the sample chamber under a He atmosphere at 220 K.

Physical Methods: Magnetic and Photomagnetic Studies. Magnetic and photomagnetic measurements were obtained using a Quantum Design MPMS-XL SQUID magnetometer residing at the Centre de

(12) Bleuzen, A.; Escax, V.; Ferrier, A.; Villain, F.; Verdaguer, M.; Münsch, P.; Itié, J.-P. *Angew. Chem., Int. Ed.* **2004**, *43*, 3728−3731.
(13) Escax, V.; Champion, G.; Arrio, M.-A.; Zacchigna, M.; Cartier dit Moulin, C.; Bleuzen, A. *Angew. Chem., Int. Ed.* **2005**, *44*, 4798−4801.
(14) Cartier dit Moulin, C.; Champion, G.; Cafun, J.-D.; Arrio, M.-A.; Bleuzen, A. *Angew. Chem., Int. Ed.* **2007**, *46*, 1287−1289.
(15) Bernhardt, P. V.; Bozoglian, F.; Macpherson, B. P.; Martínez, M. *Coord. Chem. Rev.* **2005**, *249*, 1902−1916.
(16) Oshio, H.; Onodera, H.; Tamada, O.; Mizutani, H.; Hikichi, T.; Ito, T. *Chem Eur. J.* **2000**, *6*, 2523−2530.
(17) Berlinguette, C. P.; Dragulescu-Andrasi, A.; Sieber, A.; Güdel, H. −U.; Achim, C.; Dunbar, K. R. *J. Am. Chem. Soc.* **2005**, *127*, 6766−6779.
(18) Berlinguette, C. P.; Dragulescu-Andrasi, A.; Sieber, A.; Galán-Mascarós, J. R.; Güdel, H.-U.; Achim, C.; Dunbar, K. R. *J. Am. Chem. Soc.* **2004**, *126*, 6222−6223.
(19) Shatruk, M.; Dragulescu-Andrasi, A.; Chambers, K. E.; Stoian, S. A.; Bominaar, E. L.; Achim, C.; Dunbar, K. R. *J. Am. Chem. Soc.* **2007**, *129*, 6104−6116.
(20) Trofimenko, S. *Inorg. Synth.* **1970**, *12*, 99−109.
(21) Trofimenko, S. *Scorpionates, The Coordination Chemistry of Polypyrazolylborate Ligands*; Imperial College Press: London, 1999; and references therein.
(22) $[(pzTp)_2Fe^{II}]$ is prepared as a precipitate in high yield via treatment of $Fe^{II}(OAc)_2\cdot 4H_2O$ with 2.1 equiv of K[pzTp] in acetonitrile under an argon atmosphere.
(23) Reger, D. L.; Grattan, T. C.; Brown, K. J.; Little, C. A.; Lamba, J. J. S.; Rheingold, A. L.; Sommer, R. D. *J. Organomet. Chem.* **2000**, *607*, 120−128.
(24) Li, D.; Clérac, R.; Parkin, S.; Wang, G.; Yee, G. T.; Holmes, S. M. *Inorg. Chem.* **2006**, *45*, 5251−5253.
(25) Andreades, S.; Zahnow, E. W. *J. Am. Chem. Soc.* **1969**, *91*, 4181−4190.

Recherche Paul Pascal. This magnetometer operates between 1.8 and 400 K, in applied ac or dc magnetic fields ranging from −7 to 7 T.

For data collected in the absence of light, polycrystalline samples of **1** were used. Crystals of **1** were isolated via filtration from the mother liquor and left to air-dry (at 300 K) on a filter paper for less than 5 min. A briefly dried sample of **1** (23.08 mg) was placed into a plastic bag, inserted into a SQUID straw, and introduced directly into the sample chamber at 100 K (He atmosphere) without purging to avoid possible solvent loss. When the sample chamber temperature became constant (100 K) the magnetometer was purged in preparation for subsequent measurements. Magnetic data were corrected for the diamagnetism of the sample holder (plastic bag) and **1**. Diamagnetic correction for **1** was estimated using Pascal's constants.[26]

The photomagnetic irradiation of samples utilized a 150 W halogen/tungsten lamp (LEICA CLS 150XD) that was directed into the magnetometer cavity via an optical fiber. Finely ground crystals of **1** (1.25, 1.96, 3.27, and 2.81 mg) were packed into a ca. 10 mg capacity Teflon cup (3 mm diameter) in direct contact with the optical fiber (on top of cup). The residual magnetic signal of the Teflon sample holder was previously determined and found to be of the same magnitude as the instrumental magnetization noise; consequently no diamagnetic correction for the sample holder was applied to the raw magnetic data collected. The incident light intensity power was determined ex-situ to be 575(40) mW cm^{-2}. All temperatures were corrected for sample heating (via incident white light) relative to those obtained in the absence of light. Desexcitation of the photoinduced and quenched states have been tested without success using a variety of 5 W LED lights (Lumileds, Luxeon V) with the following effective powers and wavelengths (width at half height between parentheses): 174(3) mW cm^{-2} at 455(20) nm; 99(3) mW cm^{-2} at 470(25) nm; 52(3) mW cm^{-2} at 505(30) nm; 71(3) mW cm^{-2} at 530(35) nm.

Synthesis of $[NEt_4][(pzTp)Fe^{III}(CN)_3]$.[24] Treatment of $[(pzTp)_2Fe^{II}]$[22] (1.228 g, 2.00 mmol) (pzTp = tetra(pyrazolyl)borate) with $[NEt_4]CN$ (0.967 g, 6.20 mmol) in MeCN (40 mL) for 1 h at 50 °C afforded an orange solution, that was evacuated to dryness. The orange solid residue was dissolved into 30% aqueous H_2O_2 (30 mL) and allowed to stir for 20 h at room temperature (30 °C). *Caution: Evacuation of the mixture to dryness can cause detonation when magnetically stirred.* The yellow precipitate was collected via suction filtration, washed with cold water (2 × 5 mL), and dried under vacuum for 5 h at room temperature. Yield: 0.815 g (75.0%). Yellow crystals are obtained from dry MeCN/Et_2O mixtures after 3 days. Anal. Calcd for $C_{23}H_{32}BN_{12}Fe$: C, 50.85; H, 5.94; N, 30.94. Found: C, 50.62; H, 6.42; N, 30.83. IR (Nujol, cm^{-1}): 3147 (m), 3139 (m), 3126 (m), 2120 (s), 1501 (s), 1485 (s), 1441 (vs), 1409 (vs), 1392 (vs), 1366 (s), 1305 (vs), 1246 (m), 1204 (vs), 1188 (s), 1172 (m), 1105 (s), 1092 (m), 1081 (s), 1059 (vs), 996 (m), 923 (m), 873 (m), 858 (s), 832 (m), 809 (s), 783 (vs), 772 (vs), 760 (s), 663 (w), 618 (m), 529 (w), 479 (w), 408 (m). μ_{eff} (μ_B) = 2.35.

Synthesis of $\{[(pzTp)Fe^{III}(CN)_3]_4[Co^{II}(pz)_3CCH_2OH]_4[ClO_4]_4\}\cdot 13DMF\cdot 4H_2O$ (1). Treatment of $Co(ClO_4)_2\cdot 6H_2O$ (0.366 g, 1.00 mmol) in DMF (10 mL) with $[NEt_4][(pzTp)Fe^{III}(CN)_3]$ (0.543 g, 1.00 mmol) afforded a dark red solution that was magnetically stirred for 2 h. Addition of Et_2O (60 mL) precipitated a red oil and the supernatant was decanted; the red oil was washed with 1:8 DMF/Et_2O (45 mL) and evacuated to dryness affording a red powder. The red solid was extracted into CH_2Cl_2 (15 mL) and filtered; $(pz)_3CCH_2OH$ (0.244 g, 1.0 mmol) was added, and the red mixture was allowed to stir for 2 h. The solution was evacuated to dryness at room temperature. The red residue was dissolved into DMF (10 mL) and layered with Et_2O (40 mL), and red blocks were collected after 6 days. Yield: 0.567 g (52.9%). Anal. Calcd for $C_{143}H_{195}B_4Cl_4Co_4Fe_4N_{81}O_{37}$: C, 40.08; H, 4.59; N, 26.48. Found: C, 39.71; H, 4.74; N, 26.69. IR (Nujol, cm^{-1}): 3402 (m, br), 3144 (m), 2950 (vs), 2923 (vs), 2855 (vs), 2692 (w), 2620 (w), 2168 (s), 1659 (vs), 1517 (m), 1500 (s), 1459 (s), 1442 (s), 1410 (vs), 1388 (vs), 1337 (s), 1315 (s), 1306 (s), 1253 (m), 1230 (s), 1211 (s), 1168 (vs), 1102 (vs), 1091 (vs), 1000 (w), 968 (m), 924 (m), 874 (s), 858 (s), 809 (s), 786 (s), 770 (vs), 723 (w), 662 (m), 621 (s), 607 (m), 540 (w), 504 (w), 431 (m). UV−vis (CH_3CN): λ_{max}/nm (ϵ_M/M^{-1} cm^{-1}; T = 300 K): 440 (7077), 510 (4234).

Structure Determinations and Refinements. X-ray diffraction data for **1** were collected at various temperatures and cooling rates between 90 and 260 K on a Nonius κCCD diffractometer using Mo Kα radiation. Crystals were mounted in Paratone-N oil on glass fibers. Initial cell parameters were obtained (DENZO)[27,28] from ten 1° frames (SCALEPACK).[28] Lorentz/polarization corrections were applied during data reduction. The structures were solved by direct methods (SHELXL97),[29] and completed by difference Fourier methods (SHELXL97).[29] Refinement was performed against F^2 by weighted full-matrix least-squares (SHELXL97),[29] and empirical absorption corrections (either SCALEPACK[28] or SADABS[30]) were applied. Hydrogen atoms were found in difference maps and subsequently placed at calculated positions using suitable riding models with isotropic displacement parameters derived from their carrier atoms. Non-hydrogen atoms were refined with anisotropic displacement parameters. Atomic scattering factors were taken from the *International Tables for Crystallography Vol. C*.[31]

Results and Discussion

Synthesis, Crystallographic Studies, and Spectroscopic Characterization. Compound **1**, $\{[(pzTp)Fe^{III}(CN)_3]_4[Co^{II}(pz)_3CCH_2OH]_4[ClO_4]_4\}\cdot 13DMF\cdot 4H_2O$, was prepared[32] via treatment of equimolar quantities of $[NEt_4][(pzTp)Fe^{III}(CN)_3]$[24] (pzTp = tetrapyrazolylborate) with cobalt(II) perchlorate in *N*,*N*′-dimethylformamide, followed by the addition of 2,2,2-tris(pyrazolyl)ethanol ($tpmCH_2OH$).[23] Compound **1** crystallizes as a red cationic octanuclear complex in the monoclinic $P2_1/c$ space group. The octanuclear core of **1** consists of a slightly distorted $\{Fe_4Co_4\}$ box in which cobalt and iron centers reside in alternate corners and are linked via cyanides along the cube edges (Figure 1, left); charge balancing perchlorate anions and interstitial solvent molecules keep the cationic $\{Fe_4Co_4\}$ boxes well-separated from each other. The remaining three coordination sites on the Fe and Co centers are satisfied by facially coordinate $pzTp^-$ and $tpmCH_2OH$ ligands, respectively, affording FeC_3N_3 and CoN_6 coordination environments.

Crystallographic Studies. Crystallographic data collected for rapidly cooled crystals of **1** suggest that the metrical parameters are comparable at 260 and 90 K, respectively. At 260 K (Figure 1, left), the average Fe−C and Co−N cyanide bond distances are 1.920(8) and 2.063(7) Å, respectively, while the C−Fe−C and N−Co−N bond angles are respectively 87.8(3) and 92.5(3)° (Tables 1 and 2). Valence sum bond analysis and charge compensation indicate that the cobalt centers are high-spin and in the divalent state, while the iron centers are trivalent, forming $Co^{II}(\mu$-NC)Fe^{III} linkages; the average face (Fe1···Fe4), edge (Fe1···Co4), and body diagonal (Fe1···Co3) distances are 7.465(7), 5.108(7), and 8.887(7) Å, respectively. In comparison, the X-ray data suggests that for quickly cooled crystals of **1** (cold

(26) Kahn, O. *Molecular Magnetism*; VCH Publishers: New York, 1993.

(27) Varret, F.; Boukheddaden, K.; Codjovi, E.; Maurin, I.; Tokoro, H.; Ohkoshi, S.-I.; Hashimoto, K. *Polyhedron* **2005**, *24*, 2857−2863.
(28) Otwinowski, Z.; Minor, W. *Methods Enzymol.* **1997**, *276*, 307−326.
(29) Sheldrick, G. M. *SHELX-97. Programs for Crystal Structure Solution and Refinement*; University of Göttingen: Göttingen, Germany, 1997.
(30) Sheldrick, G. M. *SADABS- An empirical absorption correction program;* Bruker Analytical X-Ray Systems: Madison, WI, 1996.
(31) *International Tables for Crystallography, Vol. C*: Kluwer Academic Publishers: Dordrecht, The Netherlands, 1992.
(32) Li, D.; Parkin, S.; Wang, G.; Yee, G. T.; Clérac, R.; Wernsdorfer, W.; Holmes, S. M. *J. Am. Chem. Soc.* **2006**, *128*, 4214−4215.

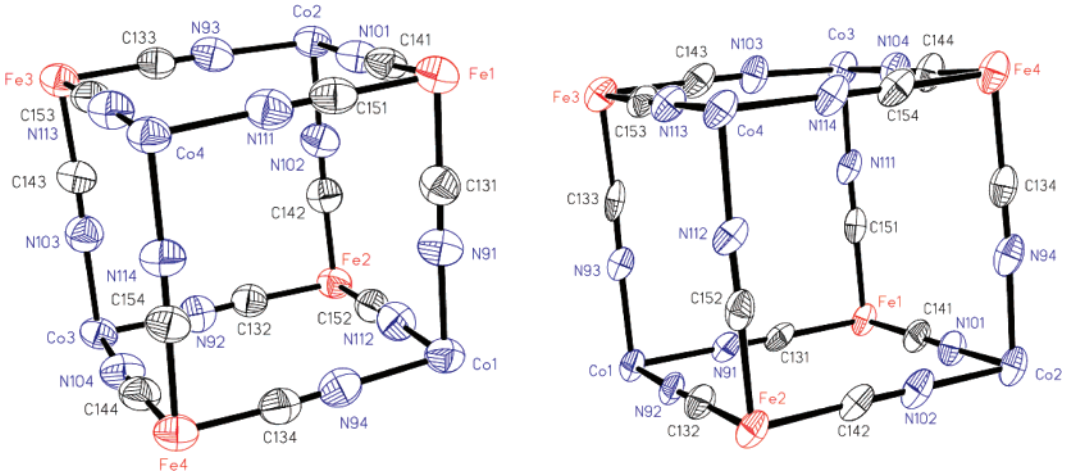

Figure 1. Truncated X-ray structures of $\{Fe(\mu\text{-}CN)_3Co\}_4$ cores present in **1** at 260 K (left) and 90 K (right). Thermal ellipsoids are at the 50% probability level and all anions, lattice solvents, hydrogen atoms, $pzTp^-$, and $tpmCH_2OH$ ligands have been eliminated for clarity.

Table 1. Crystallographic Data for **1** at Various Temperature and Cooling Rates

	260 K	300 → 90 K (quench)	300 → 90 K (1 K min^{-1})
crystal color	brick red	brick red	dark green
formula	$C_{143}H_{195}B_4Cl_4Co_4Fe_4N_{81}O_{37}$	$C_{143}H_{195}B_4Cl_4Co_4Fe_4N_{81}O_{37}$	$C_{143}H_{195}B_4Cl_4Co_4Fe_4N_{81}O_{37}$
formula wt	4284.96	4284.96	4284.96
crystal system	monoclinic	monoclinic	monoclinic
space group	$P2_1/c$	$P2_1/c$	$P2_1/c$
wavelength, Å	0.71073	0.71073	0.71073
temperature, K	260.0(6)	90.0(2)	90.0(2)
a, Å	25.2803(2)	25.2662(2)	25.0653(3)
b, Å	23.9110(2)	23.5797(2)	23.4624(3)
c, Å	35.5400(4)	35.5970(3)	34.8074(6)
α, deg	90.0	90.0	90.0
β, deg	102.2742(3)	102.4440(3)	102.3652(6)
γ, deg	90.0	90.0	90.0
V, Å^3	20992.0(3)	20709.4(3)	19995.1(5)
D_c, g cm^{-3}	1.356	1.374	1.423
Z	4	4	4
μ, mm^{-1}	0.711	0.720	0.746
$R_1{}^a$	0.0962	0.0939	0.0934
$wR_2{}^a$	0.2912	0.2757	0.2346

^{a} $I > 2\sigma(I)$, $R_1 = \Sigma||F_o| - |F_c||/\Sigma|F_o|$, $wR_2 = [\Sigma w(F_o^2 - F_c^2)^2/\Sigma w(F_o^2)^2]^{1/2}$

N_2 gas; 300 → 90 K) the average metal coordination spheres of these thermally quenched crystals are nearly identical to those seen at 260 K (Table 2; Supporting Information, Figure S2).[33]

However, when crystals of **1** are slowly cooled from 260 to 90 K (at 1 K min^{-1}) in the absence of light, their color changes from red to green and the average Co−N bond distance shortens by ca. 0.2 Å (Figure 1, right; Tables 1−2; Supporting Information, Figure S2).[33] These slowly cooled crystals (90 K) exhibit (i) Co−N bond distances between 1.892(7) and 1.915(7) Å [1.905(7) Å avg] and are in the range expected for $Co^{III}{}_{LS}$-N units; (ii) Fe−C distances that range from 1.880(8) to 1.92(1) Å [1.90(1) Å avg] and are similar to those in the 260 K structure, despite a formal iron oxidation and spin state change (e.g., $Fe^{III}{}_{LS} \rightarrow Fe^{II}{}_{LS}$).[17,18,34,35] The $\{Fe_4Co_4\}$ core is slightly compressed in comparison to the 260 K structure, and average face (Fe2···Fe4), edge (Fe2···Co2), and body diagonal (Fe2···Co3) distances of 7.018(8), 4.963(8), and 8.583(8) Å are found,

(33) See the Supporting Information.

Table 2. Selected Bond Distances (Å) and Angles (deg) for **1**

	260 K	300 → 90 K (rapid)	300 → 90 K (1 K min^{-1})
Fe1−C131	1.939(8)	1.924(8)	1.907(9)
Fe1−C141	1.910(7)	1.937(9)	1.905(8)
Fe1−C151	1.908(8)	1.921(7)	1.90(1)
Fe1−N11	1.952(6)	1.967(6)	2.012(6)
Fe1−N31	1.971(6)	1.963(5)	1.999(7)
Fe1−N51	1.973(6)	1.963(6)	1.994(7)
Co1−N91	2.061(6)	2.067(6)	1.894(7)
Co1−N94	2.066(7)	2.067(6)	1.892(7)
Co1−N112	2.043(7)	2.075(5)	1.910(6)
Fe1···Co1	5.132(7)	5.131(6)	4.951(6)
Fe···Co	8.88(4)	8.90(2)	8.57(2)
C131−Fe1−C141	87.3(3)	86.8(3)	90.1(3)
C131−Fe1−C151	86.4(3)	86.9(3)	88.9(3)
C141-Fe1−C151	88.4(3)	88.4(3)	90.3(3)
N91−Co1−N94	93.7(2)	92.4(2)	90.9(3)
N91−Co1−N112	92.2(2)	92.8(2)	90.9(3)
N94−Co1−N112	92.2(2)	92.3(2)	92.2(3)

respectively. Although the space group remains the same for both temperatures ($P2_1/c$), a phase transition at 255 K was nevertheless confirmed by the presence of an endothermic peak [+56(4) kJ mol^{-1}] in the differential scanning calorimetry (DSC) data (Supporting Information, Figure S1).[33] These temperature-dependent structural variations seen in crystals of **1** suggest that intramolecular electron transfer converts $Fe^{III}{}_{LS}(\mu\text{-}CN)Co^{II}{}_{HS}$ units into $Fe^{II}{}_{LS}(\mu\text{-}CN)Co^{III}{}_{LS}$ ones.

Spectroscopic Characterization. Additional support for this intramolecular electron-transfer hypothesis can be found in temperature dependent infrared (IR) spectroscopy studies of **1** (Figure 2) conducted between 300 and 77 K. Indeed at room temperature, the cyano stretching absorption (ν_{CN}) in **1** is shifted to higher energy (2168 cm^{-1}) relative to those in $[NEt_4][(pzTp)Fe^{III}(CN)_3]$ (2115 cm^{-1}) and $[NEt_4]_2[(pzTp)Fe^{II}(CN)_3]$[33] (2069 and 2050 cm^{-1}), confirming the presence of bridging cyanides within $Fe^{III}{}_{LS}(\mu\text{-}CN)Co^{II}{}_{HS}$ linkages.[17−19] Between 250 and 190 K the high-energy ν_{CN} (2168 cm^{-1}) stretch disappears with decreasing temperature as new low-energy stretches grow in

(34) Bernhardt, P. V.; Bozoglian, F.; Macpherson, B. P.; Martínez, M.; Merbach, A. E.; González, G.; Sienra, B. *Inorg. Chem.* **2004**, *43*, 7187−7195.
(35) Bernhardt, P. V.; Bozoglian, F.; Macpherson, B. P.; Martínez, M.; González, G.; Sienra, B. *Eur. J. Inorg. Chem.* **2003**, 2512−2518.

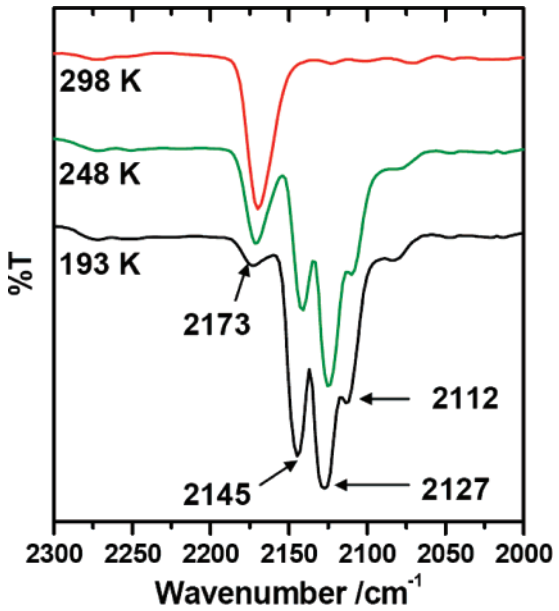

Figure 2. Infrared spectra of **1** at 298 (red), 248 (green), and 193 K (black).

intensity between 2150 and 2100 cm^{-1}. These new ν_{CN} absorptions (2112, 2127, 2145 cm^{-1}) are likely due to the formation of $Fe^{II}_{LS}(\mu\text{-CN})Co^{III}_{LS}$ units via electron transfer and are in the energy range expected for cyanometalate compounds containing Fe^{II}_{LS} centers.[7] Moreover, these temperature-induced changes in the infrared spectra of **1** are completely reversible upon warming samples above ca. 248 K, indicating that the bonding and/or electronic environments of the cyanide ligands change consistently with the transformation of $Fe^{II}_{LS}(\mu\text{-CN})Co^{III}_{LS}$ units (T < 248 K) into $Fe^{III}_{LS}(\mu\text{-CN})Co^{II}_{HS}$ ones (T > 248 K, Figure 2).

Further experimental support for intramolecular electron transfer in **1** is found in the temperature dependence of the UV−visible electronic spectra in both solution (in CH_3CN) and solid states (as Nujol mulls; Supporting Information, Figures S3 and S4).[33] At 298 K solutions of **1** exhibit a broad and intense absorption at 440 nm (ϵ_M = 7077 M^{-1} cm^{-1}) that is ascribed as a spin- and Laporte-allowed ligand-to-metal charge-transfer transition. A shoulder at 510 nm (ϵ_M = 4234 M^{-1} cm^{-1}) is also detected and is tentatively assigned as a metal-to-metal charge-transfer transition (Supporting Information, Figure S3).[1,3−18] Solid-state spectra collected between 300 and 77 K confirm that facile electron transfer occurs at temperatures below ca. 250 K in **1**. For example at 223 K, the absorption at ca. 420 nm decreases in intensity as a new one appears at ca. 670 nm (Supporting Information, Figure S4).[33] These absorptions are close to those exhibited by a series of photoresponsive Co/Fe Prussian blues.[5,6]

Accordingly, the solid-state reflectivity spectra collected under white light irradiation between 280 and 50 K confirm that the optical properties of **1** change with temperature (Figure 3, left).[33] As the temperature is lowered from 280 to 160 K, a broad absorption appears at ca. 700 nm. The most intriguing aspect of these optical measurements can be seen when comparing the 50 and 280 K spectra; *they are nearly identical*. Further investigation of this unusual behavior is more clearly seen in plots of the surface reflectivity at 700 nm as a function of temperature (Figure 3, right). At 700 nm, the reflectivity rapidly decreases between 280 and 150 K, but quickly returns to values nearly identical to those seen at 300 K. This reproducible behavior is probably associated with light-induced conversion (below ca. 180 K) of $Fe^{II}_{LS}(\mu\text{-CN})Co^{III}_{LS}$ units into Fe^{III}_{LS}-Co^{II}_{HS} pairs, while at higher temperatures (between 200 and 250 K) the $Fe^{III}_{LS}(\mu\text{-CN})Co^{II}_{HS}$ units are thermally transformed into Fe^{II}_{LS}-Co^{III}_{LS} pairs. Such behavior has been observed in X-ray and IR studies of **1** and is reminiscent of several photoresponsive iron(II) spin-crossover complexes.[36,37]

Magnetic Studies. To further investigate the apparent intramolecular electron transfer and spin-state changes in **1**, we measured the magnetic properties as a function of temperature and light exposure. The temperature dependence of the susceptibility (χ) has been investigated using a commercial SQUID magnetometer (Quantum Design MPMS-XL). Between 300 and 265 K the χT product remains nearly constant (12.7 cm^3 K mol^{-1}) in excellent agreement with the value expected for a 4:4 ratio of magnetically isolated low-spin Fe^{III} (S = $^1/_2$, $g \approx$ 2.7) and high-spin Co^{II} (S = $^3/_2$, $g \approx$ 2.3) centers (Figure 4, left). Slowly decreasing the temperature (0.4 K min^{-1}) from 265 to ca. 255 K affords a monotonic decrease in the χT values, quickly approaching 0.57 cm^3 K mol^{-1} at 200 K. Surprisingly, repeated cycling of the temperature between 200 and 270 K (at 0.2 to 1 K min^{-1}) leads to perfectly reproducible data without detectable thermal hysteresis. As already suggested by the structural, spectroscopic, and optical measurements of **1**, this magnetic feature is clearly associated with an electron-transfer process that transforms Fe^{III}_{LS} (S = $^1/_2$) and Co^{II}_{HS} (S = $^3/_2$) metal ions into diamagnetic Fe^{II}_{LS} and Co^{III}_{LS} (S = 0) centers. In addition the small residual paramagnetism seen below ca. 200 K is likely due to Fe^{III}_{LS} and Co^{II}_{HS} ions (ca. 4.5%) that were trapped either during the structural-electronic transition or via crystallographic defects present in crystals of **1**.

To probe the possibility that high temperature paramagnetic states can be trapped, samples were rapidly cooled (30 K min^{-1}) from 300 to 5 K, and their magnetic data collected. As judged from the χT vs T data, rapidly quenched samples exhibit χT values that are comparable to those seen for the high-temperature phase (Figure 4, left), suggesting that the electron-transfer process was thermally frozen. However below 16 K, this quenched metastable phase exhibits antiferromagnetic three-dimensional order (associated with sharp decrease of χT below ca. 30 K; Supporting Information, Figure S5) that is probably induced by magnetic interactions between adjacent magnetic $\{Fe^{III}_4Co^{II}_4\}$ complexes.[38] Furthermore, this apparent antiferromagnetic phase is identical to the one seen for samples of **1** after white light irradiation (below 100 K) of the thermodynamic and diamagnetic $\{Fe^{II}_4Co^{III}_4\}$ state (Supporting Information, Figure S6).[33] After irradiation at 30 K for 20 h, photoinduced electron transfer is nearly complete (Supporting Information, Figure S7) suggesting that the diamagnetic $\{Fe^{II}_4Co^{III}_4\}$ complexes have been transformed into paramagnetic $\{Fe^{III}_4Co^{II}_4\}$ ones (Figure 4, left).[33]

These results strongly suggest that intramolecular electron transfer observed for **1** at 250 K can reversibly convert

(36) Desaix, A.; Roubeau, O.; Jeftic, J.; Haasnoot, J. G.; Boukheddaden, K.; Codjovi, E.; Linarès, J.; Noguès, M.; Varret, F. *Eur. Phys. J. B* **1998**, *6*, 183−193.
(37) Létard, J.-F.; Guionneau, P.; Rabardel, L.; Howard, J. A. K.; Goeta, A. E.; Chasseau, D.; Kahn, O. *Inorg. Chem.* **1998**, *37*, 4432−4441.
(38) The antiferromagnetic phase will be described in more detail in a subsequent manuscript.

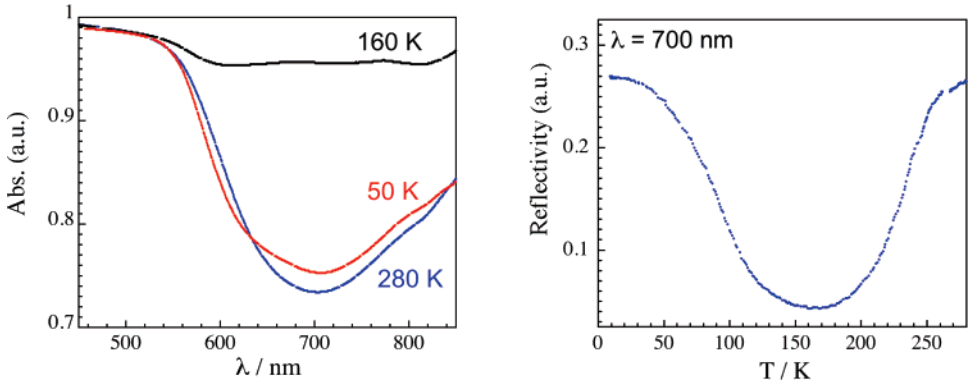

Figure 3. Surface absorption spectra of **1** at 50 (red), 160 (black), and 280 (blue) K (left). Temperature dependence of surface reflectivity of **1** at 700 nm [white light irradiation, 90(10) mW cm^{-2}] (right). All data collected between 280 and 10 K at cooling/heating rates of 3 K min^{-1}.

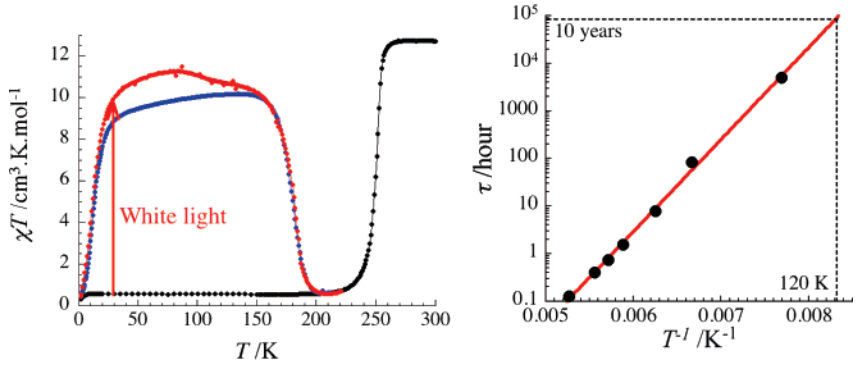

Figure 4. χT vs T data (with $\chi = M/H$ at 0.4 K/min) for **1** between 1.8 and 300 K ($H_{dc} = 1$ T) before (black dots) and after (red dots) halogen white light irradiation at 30 K and 575(40) mW cm^{-2} for 20 h (left). χT vs T data (blue dots) after thermal quenching of **1** from 300 to 5 K. The lines are guides for the eye. Relaxation time (τ) vs T^{-1} emphasizing thermally activated behavior of τ in **1** (red line, right).

paramagnetic $\{Fe^{III}_4Co^{II}_4\}$ complexes into diamagnetic $\{Fe^{II}_4Co^{III}_4\}$ boxes, both as a function of temperature and light. For rapidly cooled samples of **1**, it is likely that there is insufficient thermal energy to accommodate the dramatic changes in metal–ligand bond distances upon electron transfer, and a trapped $\{Fe^{III}_4Co^{II}_4\}$ state is obtained. Remarkably, gradually increasing the temperature at a rate of 0.4 K min^{-1} allows the thermally quenched metastable $\{Fe^{III}_4Co^{II}_4\}$ state to relax into the diamagnetic $\{Fe^{II}_4Co^{III}_4\}$ one, for temperatures up to an impressive 180 K; white light irradiation or thermal quenching of **1** can regenerate the intitial $\{Fe^{III}_4Co^{II}_4\}$ metastable state.[39]

The most important feature of the metastable state (obtained by thermal quench or photoirradiation) is its lifetime. Surprisingly the rate at which the χT product relaxes toward zero (the diamagnetic state) appears to be independent of how samples of **1** were quenched and are identical to the rates estimated for the decay of the photoinduced state. For example, the time it takes for the χT value to approach zero has been determined at various temperatures (Supporting Information, Figure S8),[32] and a characteristic relaxation time (τ) was estimated. As judged from the data illustrated in Figure 4 (right), τ obeys thermally activated behavior with $\tau = 2.6\ 10^{-8}\ \exp(4455/T)$, suggesting that a remarkably long relaxation time is found for **1**; samples of **1** irradiated below 100 K exhibit identical relaxation rates. *In other words, we propose that the thermally quenched and photoinduced states exhibit the same relaxation times and are identical in 1.* To our knowledge photoinduced magnetic relaxation times in Co/Fe Prussian blues have been analyzed only for $Na_{0.32}Co[Fe(CN)_6]_{0.74}\cdot 3.4H_2O$ that displays an activation energy barrier to electron transfer (Δ) of 3110(60) K and $\tau_0 = 6.7 \times 10^{-7}$ s.[11,27] The three-dimensional Prussian blue $Na_{0.32}Co[Fe(CN)_6]_{0.74}\cdot 3.4H_2O$ exhibits $\tau \sim 33$ h while the molecular analogue **1** exhibits a surprisingly long relaxation lifetime of $\tau \sim 10$ yr at 120 K.

Conclusions. In summary, we have demonstrated for the first time that a soluble molecular analogue of three-dimensional Fe/Co Prussian blues can exhibit both thermally and photoinduced reversible electron transfer. Evidence in support of this claim was obtained via extensive X-ray crystallographic, spectroscopic, and magnetic characterization methods. The data suggest that a well-defined octanuclear complex exhibits efficient electron transfer below 250 K, converting paramagnetic $\{Fe^{III}_4Co^{II}_4\}$ cages into diamagnetic $\{Fe^{II}_4Co^{III}_4\}$ ones. Upon electron-transfer dramatic changes in molecular structure as well as the electronic, optical, and magnetic properties are observed in **1** and can be triggered via temperature changes and/or exposure to light. We postulate that the extremely long relaxation times of the thermally and/or photogenerated metastable state may be a useful property that can be utilized in the construction of functional molecule-based electronic devices.[24,40,41]

(39) Desexcitation of the photoinduced state has been attempted without success using narrow-band irradiation between 420 and 550 nm.

(40) Li, D.; Parkin, S.; Wang, G.; Yee, G. T.; Clérac, R.; Holmes, S. M. *Inorg. Chem.* **2006**, *45*, 7569–7571.
(41) Tyagi, P.; Li, D.; Holmes, S. M.; Hinds, B. J. *J. Am. Chem. Soc.* **2007**, *128*, 4929–4938.

Acknowledgment. S.M.H. gratefully acknowledges the Kentucky Science and Engineering Foundation (Grants KSEF-621-RDE-006 and KSEF-992-RDE-008) and National Science Foundation (CAREER CHE-0645414) for financial support. R.C. and C.M. thank MAGMANet (NMP3-CT-2005-515767), the CNRS, the University of Bordeaux 1, and the Conseil Régional d'Aquitaine for financial support.

Supporting Information Available: X-ray crystallographic data in CIF format and additional spectroscopic and magnetic data. This material is available free of charge via the Internet at http://pubs.acs.org.

JA0757632